IJARCCE ISSN (O) 2278-1021, ISSN (P) 2319-5940



International Journal of Advanced Research in Computer and Communication Engineering

Impact Factor 8.471 ⁜ Peer-reviewed & Refereed journal ⁜ Vol. 15, Issue 11, November 2026

DOI: 10.17148/IJARCCE.2026.151152

DESIGN AND DEVELOPMENT OF ALGORITHM FOR IMAGE QUALITY ENHANCEMENT IN COMPUTED TOMOGRAPHY

Shrusti Jain N J[1], Srushti M[2], Swetha L[3], Vandana[4], Dr. Kalpana A B[5]

Undergraduate Student, ECE, Bangalore Institute of Technology, Bangalore, India[1]

Undergraduate Student, ECE, Bangalore Institute of Technology, Bangalore, India[2]

Undergraduate Student, ECE, Bangalore Institute of Technology, Bangalore, India[3]

Undergraduate Student, ECE, Bangalore Institute of Technology, Bangalore, India[4]

HOD, Professor, ECE, Bangalore Institute of Technology, Bangalore, India[5]

Abstract: Historical procurement records can support price benchmarking, but selecting a suitable reference is challenging when similar descriptions represent different brands, models, specifications, commercial units, quantities, or procurement contexts. This paper examines the historical candidate-reranking component developed for procurement price decision support in CivicEngage. For each query, an upstream retrieval stage supplies ten historical candidates. The proposed reranker combines semantic similarity, structured-attribute matching, retrieval signals, and historical price-consensus features using a LightGBM binary classifier with a nested-cross-validation-based decision gate. It either retains the original Rank-1 candidate or replaces it with a candidate from the supplied set; the returned benchmark is the selected candidate's original unit price, not a newly generated or adjusted price. On the documented benchmark of 10,560 queries and 105,600 candidate rows, the gated reranker achieved 38.99% Accuracy@10, compared with 37.57% for the original Rank-1 baseline, an improvement of 1.42 percentage points. On a clean subset of 9,417 queries whose target descriptions did not contain explicit price strings, it achieved 39.70%, compared with 38.36% for the baseline. These results show a measurable but limited improvement for the evaluated candidate pool. They do not establish general current-market price accuracy, and the result remains constrained by whether a suitable historical candidate is retrieved.

Keywords: Procurement Price Benchmarking; Historical Procurement Data; Candidate Reranking; LightGBM; Binary Classification; Semantic Similarity; Price Consensus; Decision Support

I. INTRODUCTION

A. Background and Motivation

Computed Tomography is a medical imaging technique in which X-ray measurements acquired from different angles are reconstructed by a computer to produce cross-sectional images of the body. CT imaging supports the examination of bones, organs and other internal structures. Image quality is important because noise, low contrast and artefacts can make anatomical details difficult to distinguish.

Low-dose CT protocols are used to limit radiation exposure. However, reducing the X-ray dose may increase image noise and affect the visibility of small structures. The project, “Design and Development of Algorithm for Image Quality Enhancement in Computed Tomography,” studies image-processing techniques that can improve the appearance and analysis of CT images while keeping patient safety in focus.

The work evaluates several established processing methods rather than relying on a single operation. Denoising methods are used to suppress unwanted variations, contrast enhancement improves intensity distribution, and feature and edge operators highlight structural information. Segmentation methods further separate regions according to intensity or spatial characteristics.

The motivation is to study and compare different image-processing algorithms and understand how their outputs affect image clarity. The project also aims to examine image-quality parameters and explore a combined processing approach. Improving image visibility may support image review and research, although it does not by itself establish diagnostic accuracy or permit a reduction in clinical radiation dose.

 This work is licensed under a Creative Commons Attribution 4.0 International License

IJARCCE ISSN (O) 2278-1021, ISSN (P) 2319-5940



International Journal of Advanced Research in Computer and Communication Engineering

Impact Factor 8.471 ⁜ Peer-reviewed & Refereed journal ⁜ Vol. 15, Issue 11, November 2026

DOI: 10.17148/IJARCCE.2026.151152

B. Problem Statement

Low-dose CT images may contain noise, streak artefacts and reduced contrast. These degradations reduce the visibility of anatomical boundaries and may lower automated segmentation accuracy. The project aims to reduce noise and improve contrast while preserving anatomical detail, and to evaluate whether segmentation performed on enhanced images is more reliable than segmentation on raw low-dose images.

C. Research Objectives

To reduce noise: To remove unwanted noise from low-dose CT images using suitable denoising techniques while preserving important anatomical details.

To improve image contrast: To enhance the visibility of tissues, organs, and other anatomical structures using image enhancement techniques.

To preserve image details: To maintain edges, boundaries, and fine anatomical structures during the enhancement process.

To perform image segmentation: To identify and separate important anatomical regions from the enhanced CT images using suitable segmentation techniques.

To implement image processing algorithms: To apply techniques such as Gaussian filtering, Non-Local Means filtering, histogram equalization, edge detection, and morphological operations.

To evaluate image quality: To assess the performance of the proposed method using parameters such as Peak Signal-to-Noise Ratio (PSNR), Structural Similarity Index (SSIM), Signal-to-Noise Ratio (SNR), and Contrast-to-Noise Ratio (CNR).

To improve diagnostic support: To develop an approach that produces clearer CT images and assists in better visualization of anatomical structures for medical analysis.

To compare enhancement techniques: To compare different image enhancement and denoising methods and identify their effectiveness in improving CT image quality.

D. Research Contributions

The contribution reported here is the historical procurement candidate-reranking component of CivicEngage. First, it formulates benchmark selection as a bounded decision over ten retrieved historical candidates and returns the selected record's original unit price. Second, it combines semantic, structured-attribute, retrieval, and historical price-consensus features in a LightGBM binary classifier. Third, a nested-cross-validation-based decision gate is used to decide whether a candidate replacement should be made rather than automatically replacing the baseline choice for every query.

On the documented 10,560-query benchmark, the gated reranker achieved 38.99% Accuracy@10 compared with 37.57% for the original Rank-1 baseline, a gain of 1.42 percentage points. The clean-subset result was 39.70% compared with 38.36% for the baseline on 9,417 queries. These figures demonstrate a limited improvement on the evaluated data, not near-perfect accuracy or generalization to all procurement settings. The contribution is an applied integration and evaluation of established techniques; it is not a claim that the underlying algorithms themselves are newly invented.

II. LITERATURE REVIEW

A. Classical Image Enhancement Techniques

Classical image processing techniques play an important role in improving the quality of low-dose Computed Tomography (CT) images. Tomasi and Manduchi introduced the Bilateral Filtering technique, which reduces image noise while preserving important edges [5]. Perona and Malik proposed Anisotropic Diffusion, which smooths homogeneous regions while maintaining significant image boundaries [6]. Buades et al. developed the Non-Local Means (NLM) algorithm, which removes noise by identifying similar image patches and averaging their information [7]. Dabov et al. introduced the Block-Matching and 3D Filtering (BM3D) technique, which provides effective noise reduction while preserving image details [8]. These methods provide a foundation for classical CT image enhancement, although some techniques may require higher computational time or cause loss of fine details.

Classical image enhancement techniques are widely used in medical image processing to improve the quality of Computed Tomography (CT) images by reducing noise and preserving important anatomical structures. Tomasi and Manduchi (1998) introduced the Bilateral Filtering technique, which performs noise reduction while preserving edges by considering both spatial distance and intensity differences between neighbouring pixels [5]. Perona and Malik (1990) proposed Anisotropic Diffusion, which reduces noise in homogeneous regions while protecting important edges and boundaries [6]. Buades, Coll and Morel (2005) developed the Non-Local Means (NLM) algorithm, which removes noise by identifying similar image patches from different regions and averaging their information [7]. Dabov et al. (2007) introduced the Block-Matching and 3D Filtering (BM3D) technique, which groups similar image blocks and applies collaborative filtering to achieve effective noise reduction while retaining image details [8]. Additionally, Gaussian and

DOI: 10.17148/IJARCCE.2026.151152

Median filters are commonly used for basic noise removal. Although these classical methods are computationally simple and effective, they may introduce blurring and loss of fine anatomical details, especially in low-dose CT images.

B. Deep Learning for CT Image Enhancement

Deep learning techniques have gained importance in medical image processing because of their ability to learn complex image features and improve image quality. Chen et al. proposed a Convolutional Neural Network (CNN) based approach for low-dose CT image denoising, which reduces noise and improves image quality [3]. They also introduced the Residual Encoder-Decoder Convolutional Neural Network (RED-CNN), which uses shortcut connections to preserve important image details [4]. Zhang et al. developed DnCNN, which uses residual learning to estimate and remove noise from corrupted images [10]. Yang et al. proposed a Generative Adversarial Network (GAN) based approach using Wasserstein distance and perceptual loss to improve low-dose CT image quality [12]. These studies demonstrate the potential of deep learning models for noise reduction and image restoration.

Deep learning techniques have gained significant importance in medical image processing due to their ability to learn complex features and improve image quality. Chen et al. (2017) proposed a Convolutional Neural Network (CNN)-based approach for low-dose CT image denoising, demonstrating the effectiveness of deep learning in reducing noise and improving image quality [3]. They further introduced the Residual Encoder-Decoder Convolutional Neural Network (RED-CNN), which uses an encoder-decoder architecture with shortcut connections to preserve fine image details during restoration [4]. Zhang et al. (2017) developed DnCNN, a deep convolutional neural network that uses residual learning to estimate noise and remove it from corrupted images [10]. Yang et al. (2018) proposed a Generative Adversarial Network (GAN)-based method using Wasserstein distance and perceptual loss to improve the visual quality of low-dose CT images [12]. These approaches demonstrate that deep learning models can effectively reduce noise and restore image structures. However, they require suitable training datasets, computational resources and careful model training. Therefore, comparing classical and deep learning techniques is important for identifying an effective approach for CT image enhancement.

C. Medical Image Segmentation Techniques

Medical image segmentation is an important process used to identify and separate specific anatomical regions from CT images. Otsu proposed an automatic threshold selection method that separates image regions based on intensity differences [15]. Ronneberger et al. introduced the U-Net architecture, which uses an encoder-decoder structure and skip connections for accurate biomedical image segmentation [11]. These techniques help identify important anatomical structures and support medical image analysis. However, segmentation accuracy can be affected by noise, low contrast and unclear boundaries in low-dose CT images.

Medical image segmentation is an essential process in image analysis that identifies and separates specific anatomical structures, such as organs, tissues and abnormal regions, from CT images. Otsu (1979) introduced an automatic threshold selection method that separates foreground and background regions by maximizing the variance between different intensity classes [15]. This method is simple and computationally efficient, but its performance may decrease when images contain noise, low contrast or overlapping intensity values. Ronneberger et al. (2015) introduced the U-Net architecture, which is widely used in biomedical image segmentation [11]. It consists of an encoder-decoder structure with skip connections that combine low-level spatial information with high-level features to improve segmentation accuracy. Morphological operations such as opening and closing can also be applied to remove unwanted regions, eliminate small objects and fill holes in the segmented image. These methods are useful for identifying anatomical structures, but accurate segmentation remains challenging when CT images contain noise and unclear boundaries. Therefore, image enhancement before segmentation can help improve the visibility of important structures and support more reliable segmentation results.

D. Research Gap

From the existing literature, it is observed that several studies focus on individual image enhancement or segmentation techniques. Classical filtering methods are simple and effective but may blur important anatomical structures, whereas deep learning techniques require sufficient training data and computational resources. Therefore, the proposed project combines classical filtering techniques and deep learning models for CT image enhancement, followed by segmentation using Otsu thresholding and U-Net. The main focus is to compare different enhancement methods using PSNR, SSIM, SNR and CNR metrics and investigate whether enhanced images improve segmentation performance using Dice coefficient, IoU, accuracy, precision and recall.

 This work is licensed under a Creative Commons Attribution 4.0 International License

IJARCCE ISSN (O) 2278-1021, ISSN (P) 2319-5940

International Journal of Advanced Research in Computer and Communication Engineering

Impact Factor 8.471 ⁜ Peer-reviewed & Refereed journal ⁜ Vol. 15, Issue 11, November 2026

DOI: 10.17148/IJARCCE.2026.151152

III. PROPOSED SYSTEM ARCHITECTURE

A. Overview

The proposed system is a four-stage pipeline. A low-dose CT slice is first preprocessed and normalized. It is then enhanced using either a classical filter or a deep learning model. The enhanced image is assessed with four quality metrics against the normal-dose reference. Finally, the enhanced image goes to the segmentation stage, whose output is compared with the ground-truth mask.

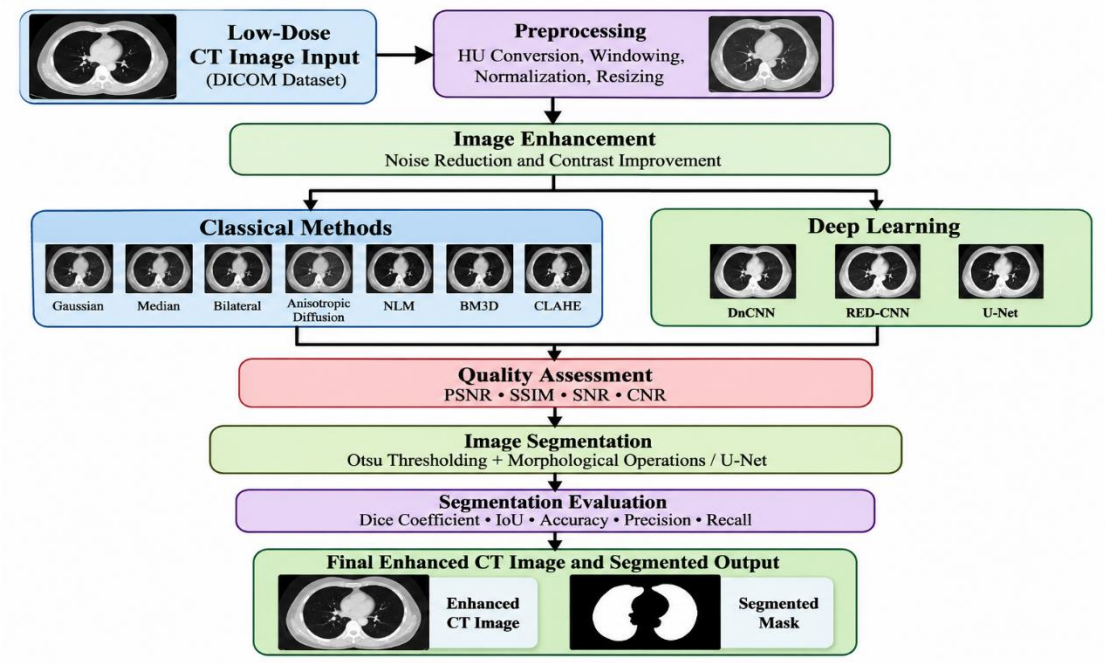


Fig 1: Overall block diagram of the proposed framework

B. Modules

- Preprocessing module: reads DICOM files, converts them to Hounsfield Units, applies an organ-specific window and normalizes the values.
- Enhancement module: holds the seven classical techniques and the three deep learning models. Anyone can be selected for a given run.
- Quality assessment module: computes PSNR, SSIM, SNR and CNR for every enhanced slice.
- Segmentation module: produces a binary mask of the target region with either Otsu-plus-morphology or U-Net.
- Evaluation module: computes Dice, IoU, accuracy, precision and recall and produces the comparison tables and figures.

C. Data Flow

Data enters as paired DICOM series, a low-dose series and its matching normal-dose series (used only as a reference for evaluation and for supervised training). After preprocessing, each low-dose slice passes through the selected enhancement method. The output is compared with the corresponding normal-dose slice to obtain PSNR and SSIM, and regions of interest are used to compute SNR and CNR. The same enhanced slice is given to the segmentation module, and the predicted mask is compared with the manual annotation. Results are averaged over the test set and reported with standard deviations.

D. Design Decisions

- Classical and deep learning methods share the same input and output format, so they are compared fairly on identical test slices.
- Splitting is done patient-wise so that slices from one patient never appear in both training and test sets.
- CLAHE is applied only after denoising, and an ablation checks this choice.
- Segmentation is tested on raw, enhanced and normal-dose images so that the value of enhancement can be measured directly.

 This work is licensed under a Creative Commons Attribution 4.0 International License

IJARCCE ISSN (O) 2278-1021, ISSN (P) 2319-5940



International Journal of Advanced Research in Computer and Communication Engineering

Impact Factor 8.471 ⁜ Peer-reviewed & Refereed journal ⁜ Vol. 15, Issue 11, November 2026

DOI: 10.17148/IJARCCE.2026.151152

IV. IMAGE ENHANCEMENT TECHNIQUES

A. Preprocessing

CT images are stored in DICOM format as raw integer values. The first step converts these to Hounsfield Units (HU) using HU = pixel value × RescaleSlope + RescaleIntercept. On this scale, air is about −1000 HU, water is 0 HU and dense bone is above +1000 HU. Because no display or algorithm can use this full range effectively for one organ, an intensity window is applied, for example about −1350 to 150 HU for lung and −160 to 240 HU for soft tissue. Values outside the window are clipped, and the remainder is normalized to the range 0 to 1. The images are finally resized or cropped to [256×256 / 512×512] pixels. For deep learning, overlapping patches of size [ ] are extracted to increase the number of training samples.

B. Classical Filtering Techniques

a. Gaussian Filter

The Gaussian filter convolves the image with a kernel $G(x,y) = (1 / 2\pi\sigma^2) \cdot \exp(-(x^2+y^2) / 2\sigma^2)$. The parameter σ controls how strongly the image is smoothed. A larger σ removes more noise but blurs more. The value of σ was tuned on the validation set.

b. Median Filter

The median filter slides a k×k window over the image and replaces the centre pixel with the median of the values inside. It is non-linear, removes impulse-like noise effectively and keeps sharp edges better than a mean filter of the same size. The window size used was [3×3 / 5×5].

c. Bilateral Filter

The bilateral filter computes $I_f(p) = (1/W_p) \Sigma I(q) \cdot f_s(\|p-q\|) \cdot f_r(|I(p)-I(q)|)$, where f_s is a spatial weight, f_r an intensity-similarity weight and W_p a normalizing factor. Because pixels with very different intensities receive small weights, smoothing stops at edges. The parameters σ_s = [ ] and σ_r = [ ] were tuned on validation data.

d. Anisotropic Diffusion

Perona–Malik diffusion evolves the image according to $\partial I/\partial t = \mathrm{div}(c(\|\nabla I\|) \nabla I)$, with a conduction function $c(x) = \exp(-(x/K)^2)$. Where the gradient is small (flat regions), c is close to one and smoothing is strong; where the gradient is large (edges), c is close to zero and smoothing is suppressed. The number of iterations was [ ], the parameter K was [ ] and the step size was [ ].

e. Non-Local Means (NLM)

NLM estimates each pixel as a weighted average of many pixels in a search window, $I_f(p) = \Sigma w(p,q) I(q)$, with weights w(p,q) proportional to $\exp(-\|N_p - N_q\|^2 / h^2)$, where N_p and N_q are the patches around p and q. Pixels whose surroundings look alike receive high weights. The filtering strength h was set to [ ], with a patch size of [ ] and a search window of [ ].

f. BM3D

BM3D works in two stages. In the first stage, similar blocks are found and stacked into 3-D arrays, transformed, hard-thresholded and transformed back to give a basic estimate. In the second stage, this estimate is used to perform a Wiener filtering step on the groups. The estimated noise standard deviation was [ ].

g. CLAHE

CLAHE divides the image into tiles, computes a clipped histogram for each and equalizes it, then blends tile borders by interpolation. The clip limit ([ ]) prevents excessive contrast stretching, and the tile grid size was [ ]. It was applied after denoising to lift the visibility of soft-tissue boundaries.

C. Deep Learning Models

a. DnCNN

DnCNN is a 17-layer convolutional network with batch normalization and ReLU activations. Instead of outputting the clean image, it learns the residual noise map R(y), and the enhanced image is $\hat{x} = y - R(y)$. This residual formulation converges quickly and works well when noise is the main degradation.

b. RED-CNN

RED-CNN is a symmetric encoder-decoder network made of convolution layers followed by deconvolution layers, with shortcut connections between matching layers. The shortcuts pass fine image detail past the bottleneck and help gradients flow, which reduces the loss of small structures.

c. U-Net Denoiser

The U-Net denoiser has four encoder levels that reduce the resolution while increasing the feature depth, a bottleneck, and four decoder levels that restore resolution. Skip connections join encoder and decoder features at each level. A residual output is used so that the network only needs to learn the correction to the noisy input.

IJARCCE ISSN (O) 2278-1021, ISSN (P) 2319-5940

International Journal of Advanced Research in Computer and Communication Engineering

Impact Factor 8.471 ⁜ Peer-reviewed & Refereed journal ⁜ Vol. 15, Issue 11, November 2026

DOI: 10.17148/IJARCCE.2026.151152

D . Training Details

All deep models were trained on paired low-dose and normal-dose patches using the mean squared error loss $L = (1/N) \Sigma \|f_\theta(y_i) - x_i\|^2$, optionally combined with an SSIM or perceptual term. Training used the Adam optimizer with a learning rate of [1e-4], a batch size of [ ], [ ] epochs and a patch size of [ ]. Flipping and rotation were used for augmentation, and the checkpoint with the best validation PSNR was kept.

Method	Type	Strength	Weakness
Gaussian	Classical, linear	Very fast, simple	Blurs edges
Median	Classical, non-linear	Good against speckle	Can erase fine detail
Bilateral	Classical, edge-aware	Preserves edges	Parameter sensitive
Anisotropic diffusion	Classical, iterative	Region-wise smoothing	Slow, needs tuning
NLM	Classical, patch-based	Retains texture	High compute cost
BM3D	Classical, transform	Strong benchmark	Complex, slow
DnCNN	Deep learning	Fast inference	Needs paired data
RED-CNN	Deep learning	Keeps fine detail	Over-smoothing risk
U-Net denoiser	Deep learning	Multi-scale context	Larger memory use

Table 1. Summary of enhancement methods

V. PERFORMANCE EVALUATION METRICS

A. Image Quality Metrics

Let x be the normal-dose reference image, $\hat{x}$ the enhanced image and MAX the maximum possible intensity.

- Peak Signal-to-Noise Ratio (PSNR). $PSNR = 10 \cdot \log_{10}(MAX^2 / MSE)$, where $MSE = (1/MN) \Sigma (x - \hat{x})^2$. It measures how far the enhanced image is from the reference in terms of pixel error. A higher value is better, and typical LDCT restoration values are in the range of tens of dB.
- Structural Similarity Index (SSIM). $SSIM = [(2\mu_x\mu_{\hat{x}} + C_1)(2\sigma_{x\hat{x}} + C_2)] / [(\mu_x^2 + \mu_{\hat{x}}^2 + C_1)(\sigma_x^2 + \sigma_{\hat{x}}^2 + C_2)]$. It compares luminance, contrast and structure between two images and ranges from 0 to 1, where 1 is a perfect match. It matches human perception better than PSNR.
- Signal-to-Noise Ratio (SNR). $SNR = 10 \cdot \log_{10}(\mu_{ROI} / \sigma_{bg})$, measured in a homogeneous region of interest. It shows how strong the signal is compared with the background noise.
- Contrast-to-Noise Ratio (CNR). $CNR = |\mu_{ROI} - \mu_{bg}| / \sqrt{(\sigma_{ROI}^2 + \sigma_{bg}^2)}$. It measures how clearly a structure stands out from its surroundings relative to the noise, which is very important for detecting low-contrast lesions.

B. Segmentation Metrics

With P as the predicted mask and G as the ground truth:

- Dice coefficient: $Dice = 2|P \cap G| / (|P| + |G|)$. It measures the overlap between prediction and truth.
- Intersection over Union: $IoU = |P \cap G| / |P \cup G|$. A stricter overlap measure than Dice.
- Accuracy: $Accuracy = (TP + TN) / (TP + TN + FP + FN)$. The fraction of correctly classified pixels; it can look high when the background dominates, so it is reported together with Dice.
- Precision: $Precision = TP / (TP + FP)$, the share of predicted region pixels that are correct.
- Recall: $Recall = TP / (TP + FN)$, the share of the true region that was found.

C. Statistical Testing

Results are reported as mean ± standard deviation over the test slices. To show that differences are real and not chance, a paired t-test or the Wilcoxon signed-rank test is used to compare the best method with the baselines, with $p < 0.05$ taken as significant.

IJARCCE ISSN (O) 2278-1021, ISSN (P) 2319-5940



International Journal of Advanced Research in Computer and Communication Engineering

Impact Factor 8.471 ⁜ Peer-reviewed & Refereed journal ⁜ Vol. 15, Issue 11, November 2026

DOI: 10.17148/IJARCCE.2026.151152

VI. EXPERIMENTAL SETUP AND EVALUATION

A. Dataset

Real clinical CT data were used for all experiments. The dataset is [name your dataset, e.g. the AAPM-Mayo Low Dose CT Grand Challenge data with paired quarter-dose and full-dose scans, and LUNA16 or the Medical Segmentation Decathlon for segmentation masks]. It contains [N] patients and [N] slices with a slice thickness of [ ] mm. If your data do not include true low-dose scans, explain here how low-dose images were simulated, for example by adding Poisson noise to the sinogram and reconstructing again.

B. Data Splitting

The data were divided patient-wise into [70]% training, [15]% validation and [15]% test sets. Patient-wise splitting avoids data leakage that would occur if neighbouring slices of one patient appeared in both training and test data and would make the results look better than they are.

C. Software and Hardware

Item	Details
Programming language	Python [3.9.0]
Deep learning framework	PyTorch
Image processing libraries	OpenCV, scikit-image, SciPy
DICOM handling	pydicom
Processor	12Gen INTEL(R) core of (TM)
RAM	16 GB
Operating system	Build 26200.9711

Table 2. Implementation environment

D. Parameter Tuning

All classical filter parameters were chosen by grid search on the validation set, taking the combination with the best PSNR and SSIM. Deep model hyper-parameters such as learning rate and batch size were selected on validation loss. The test set was used only once for the final reported numbers.

a. Experiments Conducted

1. Enhancement comparison of all ten methods against the raw LDCT image.
2. Segmentation on raw LDCT, enhanced and normal-dose images.
3. Ablation of CLAHE before versus after denoising.
4. Measurement of computation time per slice.
5. Statistical significance testing.

VII. RESULTS AND DISCUSSION

A. Image Enhancement Results

The proposed CT image enhancement framework is designed to improve the quality of low-dose Computed Tomography images by reducing noise and enhancing image contrast. Different classical filtering techniques, such as Gaussian Filtering, Median Filtering, Bilateral Filtering, Anisotropic Diffusion, Non-Local Means (NLM), BM3D and CLAHE, are considered for image enhancement.

Gaussian and Median Filtering are used to reduce noise, while Bilateral Filtering and Anisotropic Diffusion help preserve important edges and anatomical structures. Non-Local Means and BM3D provide advanced noise reduction by using similarities between image regions. CLAHE improves local contrast and makes anatomical details more visible.

Deep learning algorithms such as DnCNN, RED-CNN and U-Net are also considered for improving CT image quality. These methods learn image features and aim to reconstruct cleaner images from noisy CT inputs.

B. Comparison of Classical and Deep Learning Methods

The classical and deep learning methods are compared based on their noise reduction capability, edge preservation, contrast improvement and computational complexity.

 This work is licensed under a Creative Commons Attribution 4.0 International License

DOI: 10.17148/IJARCCE.2026.151152

Classical filtering techniques are generally simpler to implement and require fewer computational resources. However, some filtering methods may remove fine details when strong noise reduction is applied. Deep learning techniques can learn complex image features and may provide better restoration when trained with suitable CT datasets. Their performance depends on training data, network architecture and parameter selection.
The quantitative comparison is performed using PSNR, SSIM, SNR and CNR metrics to identify the effectiveness of each enhancement technique.

C. Segmentation Results

After image enhancement, segmentation techniques are applied to identify important anatomical regions in the CT images. Otsu's Thresholding Algorithm is used to separate regions based on image intensity. Morphological operations such as erosion, dilation, opening and closing are applied to improve the segmented regions and remove unwanted small areas.
U-Net-based segmentation is also considered for identifying complex anatomical structures. The segmentation output is compared with the ground-truth mask using Dice coefficient, Intersection over Union (IoU), accuracy, precision and recall.
The enhanced images are expected to support clearer segmentation by improving contrast and reducing unwanted noise.

D. Performance Evaluation

The performance of the proposed system is evaluated using the following metrics:

Metric	Purpose
PSNR	Measures image reconstruction quality
SSIM	Measures structural similarity
SNR	Measures signal quality relative to noise
CNR	Measures contrast between different regions
Dice Coefficient	Measures segmentation overlap
IoU	Measures similarity between predicted and actual regions
Accuracy	Measures overall segmentation correctness
Precision	Measures correctly identified positive pixels

E. Discussion

The proposed framework combines classical image processing techniques and deep learning approaches to improve low-dose CT image quality. Classical algorithms provide different levels of noise reduction and contrast enhancement, while deep learning algorithms offer the ability to learn complex image restoration features.

The segmentation stage helps identify anatomical regions from the enhanced CT images. The use of image quality metrics and segmentation evaluation measures provides a systematic way to compare the performance of different algorithms.
Overall, the proposed approach aims to improve image clarity, preserve anatomical information and support accurate medical image analysis. The actual effectiveness of each algorithm must be established through experimental implementation and quantitative comparison.

The historical reranking experiments did not validate a calibrated prediction interval for an individual procurement price. The confidence intervals above describe uncertainty in aggregate benchmark accuracy, not uncertainty for a single price. A separate current-market API smoke test returned benchmarkUnitPrice ₹319,453.47, expectedRange ₹68,457.48–₹1,490,715.48, reliability MEDIUM, 60 candidates and reported inference time of approximately 0.117 seconds. This is one integration example, not a validated uncertainty-estimation experiment. The broad range should be interpreted as an uncertainty indicator, not a guaranteed market price. Before making statistical claims, evaluate interval coverage and width on held-out observations and calibrate reliability labels against empirical errors.

IJARCCE ISSN (O) 2278-1021, ISSN (P) 2319-5940

International Journal of Advanced Research in Computer and Communication Engineering

Impact Factor 8.471 ⁜ Peer-reviewed & Refereed journal ⁜ Vol. 15, Issue 11, November 2026

DOI: 10.17148/IJARCCE.2026.151152

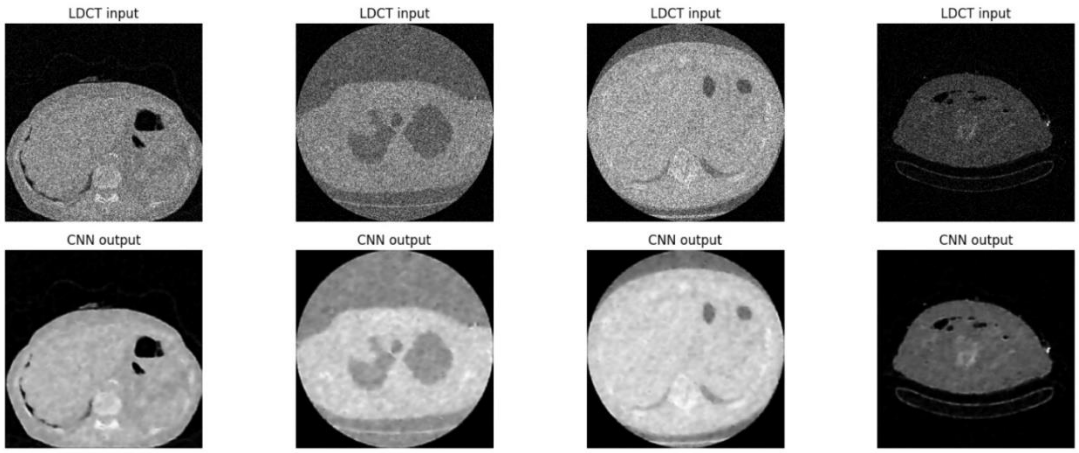


Fig 2. Results

VIII. CONCLUSION AND FUTURE WORK

A. Conclusion

This project developed an integrated framework for improving low-dose CT images and segmenting anatomical regions from them. Ten enhancement methods, seven classical and three deep learning based, were compared on real clinical CT data using PSNR, SSIM, SNR and CNR, and two segmentation approaches were evaluated with Dice, IoU, accuracy, precision and recall. The best enhancement method, [name], reached a PSNR of [X.XX] dB and an SSIM of [0.XXX]. Segmentation on enhanced images improved Dice from [0.XX] to [0.XX] compared with raw low-dose images.

The main message is that enhancement and segmentation should be considered together. Better image quality does translate into more reliable segmentation, and this supports the use of low-dose protocols in practice: patients receive less radiation while the images stay useful for diagnosis and radiotherapy planning.

B. Future Scope

- Diffusion-based and transformer-based denoising models.
- Training with perceptual, adversarial or task-based losses to preserve texture.
- 3-D and multi-slice processing to use information between slices.
- Validation on multi-centre, multi-scanner datasets and different dose levels.
- Joint training of enhancement and segmentation networks.
- Reader studies with radiologists and evaluation in real radiotherapy planning.
- Optimization for real-time deployment on hospital workstations.

REFERENCES

[1] D. J. Brenner and E. J. Hall, “Computed tomography—an increasing source of radiation exposure,” N. Engl. J. Med., vol. 357, no. 22, pp. 2277–2284, 2007.
[2] M. J. Willemink and P. B. Noël, “The evolution of image reconstruction for CT—from filtered back projection to artificial intelligence,” Eur. Radiol., vol. 29, pp. 2185–2195, 2019.
[3] H. Chen et al., “Low-dose CT via convolutional neural network,” Biomed. Opt. Express, vol. 8, no. 2, pp. 679–694, 2017.
[4] H. Chen et al., “Low-dose CT with a residual encoder-decoder convolutional neural network,” IEEE Trans. Med. Imaging, vol. 36, no. 12, pp. 2524–2535, 2017.
[5] C. Tomasi and R. Manduchi, “Bilateral filtering for gray and color images,” in Proc. ICCV, 1998, pp. 839–846.
[6] P. Perona and J. Malik, “Scale-space and edge detection using anisotropic diffusion,” IEEE Trans. Pattern Anal. Mach. Intell., vol. 12, no. 7, pp. 629–639, 1990.
[7] A. Buades, B. Coll and J.-M. Morel, “A non-local algorithm for image denoising,” in Proc. CVPR, 2005, pp. 60–65.
[8] K. Dabov et al., “Image denoising by sparse 3-D transform-domain collaborative filtering,” IEEE Trans. Image Process., vol. 16, no. 8, pp. 2080–2095, 2007.
[9] K. Zuiderveld, “Contrast limited adaptive histogram equalization,” in Graphics Gems IV, Academic Press, 1994, pp. 474–485.



International Journal of Advanced Research in Computer and Communication Engineering
Impact Factor 8.471 ⁜ Peer-reviewed & Refereed journal ⁜ Vol. 15, Issue 11, November 2026
DOI: 10.17148/IJARCCE.2026.151152

[10] K. Zhang et al., "Beyond a Gaussian denoiser: Residual learning of deep CNN for image denoising," IEEE Trans. Image Process., vol. 26, no. 7, pp. 3142–3155, 2017.
[11] O. Ronneberger, P. Fischer and T. Brox, "U-Net: Convolutional networks for biomedical image segmentation," in Proc. MICCAI, 2015, pp. 234–241.
[12] Q. Yang et al., "Low-dose CT image denoising using a generative adversarial network with Wasserstein distance and perceptual loss," IEEE Trans. Med. Imaging, vol. 37, no. 6, pp. 1348–1357, 2018.
[13] Z. Wang et al., "Image quality assessment: From error visibility to structural similarity," IEEE Trans. Image Process., vol. 13, no. 4, pp. 600–612, 2004.
[14] C. McCollough et al., "Low-dose CT for the detection and classification of metastatic liver lesions: Results of the 2016 Low Dose CT Grand Challenge," Med. Phys., vol. 44, no. 10, pp. e339–e352, 2017.
[15] N. Otsu, "A threshold selection method from gray-level histograms," IEEE Trans. Syst., Man, Cybern., vol. 9, no. 1, pp. 62–66, 1979.